Electronic Supplementary Material (ESI) for Energy & Environmental Science

Supporting Information

p-n Heterojunction Photoelectrodes Composed of Cu_2O-Loaded TiO_2 Nanotube Arrays with Enhanced Photoelectrochemical and Photoelectrocatalytic Activities

Mengye Wang[1], Lan Sun[1]*, Zhiqun Lin[2]*, Jianhuai Cai[1], Kunpeng Xie[1], Changjian Lin[1]*

EDX Study

EDX spectrum of CuO_2 loading TiO_2 NTAs prepared by by the ultrasonication-assisted S-CBD for 9 min is shown in Figure S1. The characteristic peaks of Cu, Ti and O can be clearly observed, and the atomic ratio of the Cu element was about 0.11%.

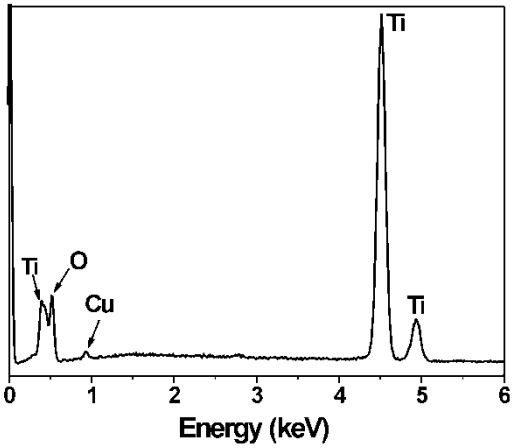

Figure S1. EDX spectrum of Cu_2O/TiO_2 NTAs.

XRD Analysis

The crystalline composition of samples was analyzed by XRD. Figure S2 shows the XRD patterns of TiO_2 NTAs before and after the deposition of Cu_2O nanoparticles. Apparently, the crystal structure of TiO_2 NTAs annealed at 450 ^oC was pure anatase phase (2θ = 25.3^o). After depositing Cu_2O, one additional diffraction peak appeared at 36.9^o, corresponding to the (111) plane of Cu_2O (JCPDS No. 05-667). There were no Cu and CuO phases present in Cu_2O/TiO_2 NTAs. Moreover, the average crystal size (D) of Cu_2O nanoparticles was 14.2 nm determined by the Scherrer's equation[1]

$$D = 0.9\lambda / (\beta \cos\theta) \quad (1)$$

where λ is the wavelength of light radiation, β is the corrected peak width at half-maximum intensity (FWHM), and θ is the corresponding peak position.

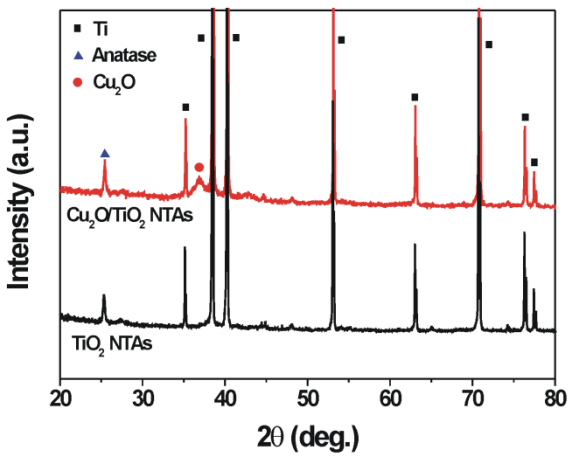

Figure S2. XRD patterns of TiO_2 NTAs and Cu_2O/TiO_2 NTAs.

PL Measurement

PL spectrum has been widely used to study the electro-optic and photoelectric properties of materials and the fate of electron-hole pairs of semiconductor particles because it can reflect the separation and recombination processes of photogenerated charge carriers in nano-sized semiconductor materials.[2] The PL spectra of anatase TiO_2 are mainly attributed to three kinds of physical origins, i.e., self-trapped excitons, oxygen vacancies, and surface states.[3, 4] Figure S3 shows the PL spectra of pure TiO_2 NTAs and Cu_2O/TiO_2 NTAs prepared by ultrasonication assisted S-CBD for 4 min. The peak at 417 nm (corresponding to 2.95 eV) can be attributed to self-trapped excitons located on the TiO_2 octahedral. The peaks at 452 nm, 469 nm, and 486 nm (corresponding to 2.74 eV, 2.64 eV, and 2.55 eV, respectively) were also observed, which are associated with the oxygen vacancies.[5-7] Cu_2O/TiO_2 NTAs exhibited a drastic quenching of PL intensity, suggesting a markedly enhanced charge separation than pure TiO_2 NTAs.

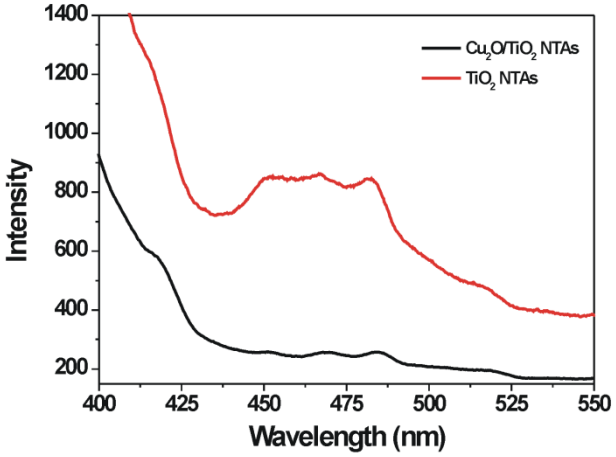

Figure S3. PL spectra of TiO_2 NTAs and Cu_2O/TiO_2 NTAs.

Stability

In order to determine whether Cu_2O photo-corrosion was existed during the photochemical and photoelectrochemical tests, XPS characterization on the Cu_2O/TiO_2 NTAs sample was performed after photochemical and photoelectrochemical measurements. The Cu 2p3/2 and Cu 2p1/2 spin-orbital photoelectrons were located at the binding energies of 932.5 eV and 952.3 eV, respectively (Figure S4A), which are known as characteristics of Cu_2O.[8] Furthermore, the Cu L_3VV Auger spectrum of the sample showed a main peak appeared at 916.9 eV (Figure S4B), which was in good agreement with Cu_2O instead of CuO and Cu.[8] Therefore, Cu_2O remained stable and photo-corrosion did not occur to Cu_2O after photochemical and photoelectrochemical measurements.

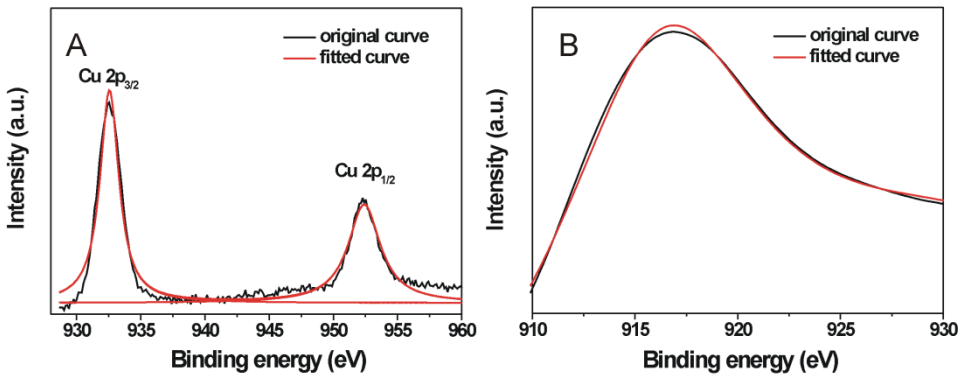

Figure S4. (A) High resolution XPS spectrum of Cu2p. (B) The Cu L_3VV Auger spectrum.

The stability of Cu_2O/TiO_2 NTAs was investigated by repeating the photoelectrocatalysis degradation of RhB for ten cycles (i.e., 50 seconds per cycle over a duration of 500 seconds) at a bias potential of 0.5 V under visible light irradiation. Cu_2O/TiO_2

NTAs were cleaned by deionized water after each experiment. Figure S5 shows that degradation of RhB was achieved nearly completely after 50 seconds in each cycle, indicating that the photoelectrocatalytic degradation efficiency under visible light was rather high and Cu_2O/TiO_2 NTAs were stable.

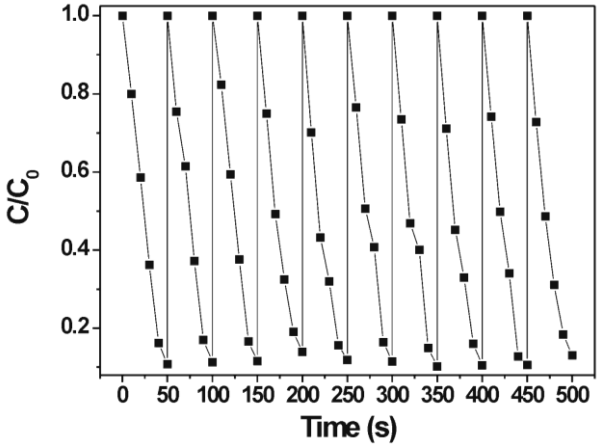

Figure S5. Cycling degradation curve for Cu_2O/TiO_2 NTAs prepared by the ultrasonication-assisted S-CBD for 4 min using 5 mg/L RhB as a probe under visible light irradiation (I_0 =130 mW cm^{-2}).

UV-vis spectra of RhB at different time intervals

Figure S6 shows the change of the absorption of RhB with the irradiation time during the photoelectrocatalytic degradation process under visible light irradiation for the first cycle and the tenth cycle. For the first cycle (Figure S6A), the removal rate of RhB pollutant was nearly complete in 50 min under the visible light irradiation. After the tenth cycle (Figure S6B), the removal rate of RhB pollutant was almost the same as that of the first cycle, implying that Cu_2O/TiO_2 NTAs have excellent stability.

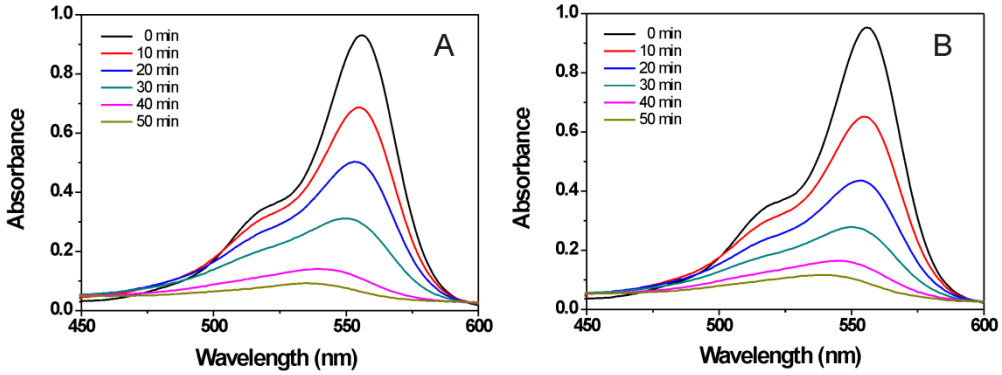

Figure S6. UV-vis spectra of RhB at different time for (A) the first cycle, and (B) the tenth cycle under the visible light irradiation.

XPS

The chemical composition of Cu_2O nanoparticles deposited on TiO_2 NTAs after 10 photoelectrocatalytic cycles was further investigated by XPS. A high-resolution XPS spectrum of Cu window showed binding energies of Cu2p doublet peaks located at 932.5 ($Cu2p_{3/2}$) and 952.4 eV ($Cu2p_{1/2}$) (Figure S7A) and the main peak was found at 916.9 eV in Cu L_3VV Auger spectrum (Figure S7B), signifying that after ten photoelectrocatalytic cycles Cu in Cu_2O/TiO_2 NTAs samples still existed in the form of Cu_2O,[8] indicating that Cu_2O nanoparticles deposited on TiO_2 nanotubes is rather stable.

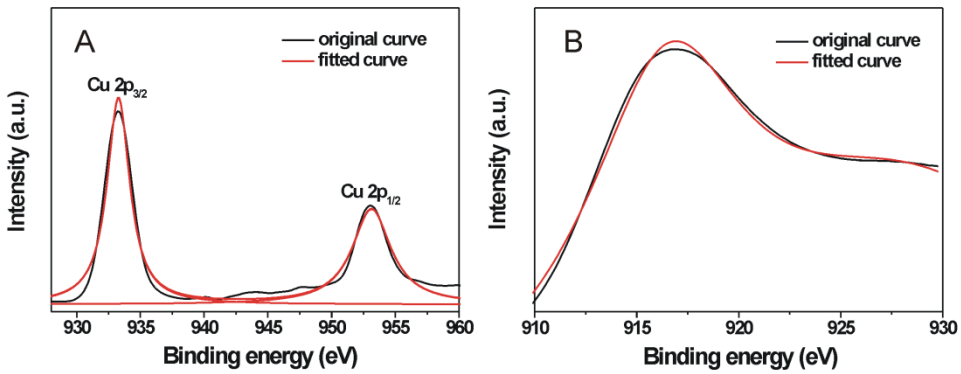

Figure S7. (A) High-resolution XPS spectrum of Cu_2O/TiO_2 NTAs after ten photoelectrocatalytic cycles. (B) The Cu L_3VV Auger spectrum.

SEM

Figure S8 shows the SEM image of surface morphology of Cu_2O/TiO_2 NTAs after ten photoelectrocatalytic cycles. Clearly, TiO_2 NTAs remained their integrity; Cu_2O nanoparticles were still attached on TiO_2 NTAs. No appreciable change in the surface morphology can be observed. This again confirmed that Cu_2O/TiO_2 NTAs possessed superior stability in the acidic solution of RhB during photocatalytic measurements.

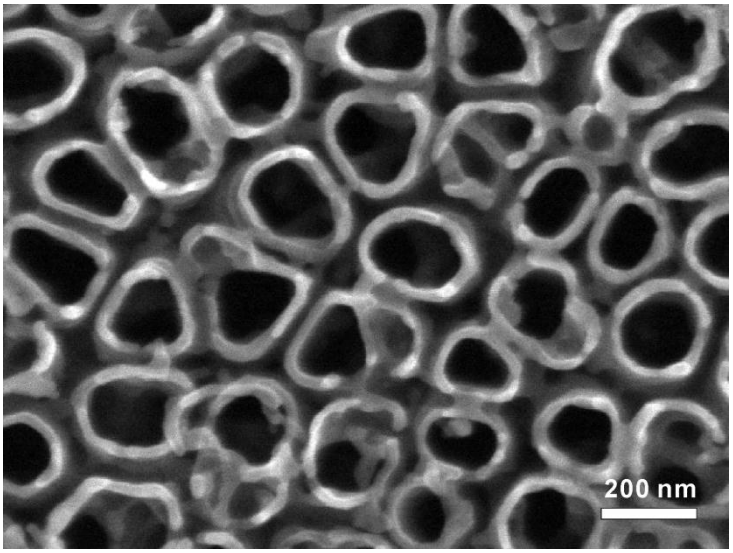

Figure S8. SEM image of Cu_2O/TiO_2 NTAs after ten photoelectrocatalytic cycles.

References

[1] P. K. Harold, E. A.Leroy, *X-ray Diffraction Procedures: For Polycrystalline and Amophous Materials*, Wiley, New York. **1974**, 618.

[2] L. Di, H. Haneda, S. Hishita, N. Ohashi, *Chem. Mater.* **2005**, *17*, 2596.

[3] T. Tachikawa, T. Majima, *Langmuir* **2009**, *25*, 7791.

[4] A. K. L. Sajjad, S. Shamaila, B. Tian, F. Chen, J. Zhang, *Appl. Catal. B- Environ.* **2009**, *91*, 397.

[5] N. Serpone, D. Lawless, R. Khairutdinov, *J. Phys. Chem.* **1995**, *99*, 16646.

[6] P. M. Kumar, S. Badrinarayanan, M. Sastry, *Thin Solid Films* **2000**, *358*, 122.

[7] T. Tachikawa, T. Majima, *J Am. Chem. Soc.* **2009**, *131*, 8485.

[8] J.F. Moulder, W.F. Stickle, P.E. Sobol, K.D. Bomben, *Handbook of X-Ray Photoelectron Spectroscopy: A Reference Book of Standard Spectra for Identification and Interpretation of XPS Data*, Perkin- Elmer Corporation, **1995**.